ANYdrive
A complete robot joint

Fully integrated

ANYdrive consists of a powerful brushless motor, a backlash-free gear, high-precision encoders, and efficient power electronics.

Absolute position sensing

Precise absolute encoders make repeated calibration of the joints unnecessary.

Programmable controller

Custom control algorithms can be implemented through the open API (coming soon).

Accurate torque control & impact robustness

The intergrated spring enables accurate torque tracking while protecting the gear from impacts.

High load bearing & hollow shaft

The robust design and hollow shaft allow for compact robot design and optimal cable routing.

Ingress-protection IP66

The ANYdrive is completey sealed against dust and water ingress.

Peak/nominal power	480 W / 180 W	Absolute joint position	17-bit, ‹0.025°
Nominal voltage	48 VDC	Joint output torque resolution	‹0.1 Nm
Peak/nominal torque	40 Nm / 15 Nm	Control modes	Position, torque, impedace,
Peak joint velocity	12 rad/s		velocity, or current control
Torque control bandwidth	›60 Hz	Communication	CAN 1 Mbit/s,
Dimensions (L x D)	93 x 80 mm		CANopen protocol,
Mass	0.9 kg		ROS integration
Max. bending moment	?? Nm		

Example applications

contact: info@anybotics.ch

D3.1 SEA with integrated electronics

March 4, 2016

1 ANYdrive - Modular joint units

ANYdrive was designed according to the following features:

- High impact robustness

- Fast motion tracking

- Low impedance force controllability

It was successfully tested and meets all the requirements. A movie documentation of the actuator performance is available here: https://youtu.be/lESsdD3o78k

1.1 Overview

ANYdrive (fig. 1(a)), the joint units of ANYmal, is a highly integrated series elastic actuator. It is built upon high torque motors and harmonic drive gears in series with a rotational spring. Joint output position and spring deflection are measured using absolute position sensors providing a position accuracy of 0.025°and a torque resolution of 8 mNm. Thanks to integrated custom motor control electronics, joint torque, position, and impedance can be directly regulated without any additional components. The corresponding command values are sent over CAN bus using CANopen standard. With a nominal voltage of 48 V, the joint reaches a speed of 12 $\mathrm{rad/s}$ and a maximal torque of 40 Nm.

1.2 Control structure

Joint torque, position and impedance control is realized as a cascaded structure that considers the motor as torque source (c.f. [10]) as illustrated in fig. 1(b). Similar to the work by Paine [11], which is also the basis of the control of Valkyrie [8], we realized a simple PID torque feedback loop with feedback friction compensation. The position PID control builds upon the torque controller as an additional cascade.

The torque controller tracks a desired torque τ^{des} by measuring the actual output torque τ and setting the desired current i^{des} accordingly. The spring deflection is calculated from the difference in the joint position θ_j and the gear position θ_g. The output torque τ is then calculated using the spring constant k. The torque controller consists of three elements, i.e. a PID controller, a feed forward term and a

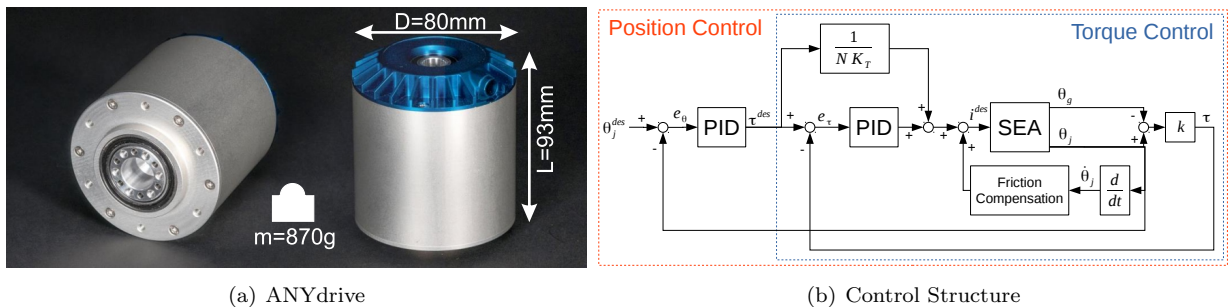(a) ANYdrive

(b) Control Structure

Figure 1: ANYdrive: Compact, compliant joint units for advanced interaction (a). Block diagram of the cascaded joint position and torque control loop. The SEA block represents the physical actuator unit including field oriented control (FOC) to apply the desired current i^{des} b)()

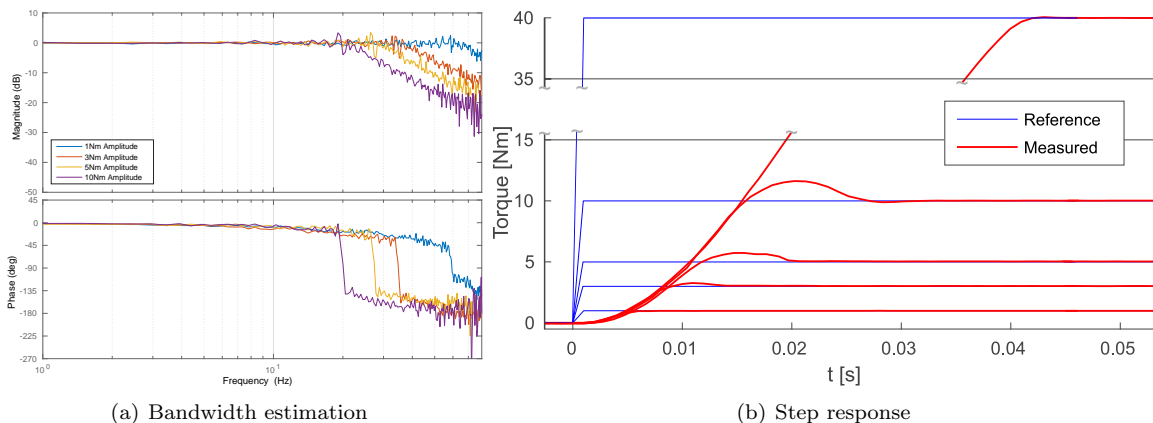(a) Bandwidth estimation

(b) Step response

Figure 2: Experimentally identified torque control transfer function indicating a bandwidth of 70 Hz (a). Torque step responses show a quick response time and low overshoot. (b)

feedback friction compensation. The feed forward term is determined from the inverse of the gear ratio N and the motor constant K_T, both typically provided in by data sheets. The friction compensation

$$i_{comp}(\dot{\theta}_j) = i_{ba}sSign(\dot{\theta}_j, \dot{\theta}_{band}) + \mu\dot{\theta}_j \tag{1}$$

takes two effects into account, namely stiction and viscous friction. Firstly the break-away current i_{ba} is modeled as Coulomb friction. To prevent undesired switching around the zero velocity point, it is implemented as simple smooth sign function

$$sSign(x, x_b) = \begin{cases} -1, & \text{if } x < x_b \\ 1, & \text{if } x > x_b \\ -1 + 2(\frac{x+x_b}{2x_b})^2(2 - \frac{x}{x_b}), & \text{otherwise} \end{cases} \tag{2}$$

Secondly, the joint velocity dependent viscous friction is linearly modeled with the friction coefficient μ. All these parameters can be experimentally identified from very few measurements.

The position controller is a PID controller that tracks a desired joint position θ_j^{des} by setting a desired torque τ^{des}. An important note is that the position gains are highly depending on the output load since there is no knowledge about the joint load in the control architecture.

1.3 Performance evaluation

The performance of ANYdrive with respect to torque and position reference tracking as well as impulsive disturbance rejection is evaluated on a single axis test bench. As illustrated in fig. 2(a), the bandwidth for low amplitudes is as high as 70 Hz. Due to motor saturation effects, the bandwidth gradually decreases to 24 Hz for 10 Nm amplitude. These performance values are substantially higher than what was achieved with our previous system [12] and about the same as in Valkyrie [8]. Interestingly, this high performance was achievable without a disturbance observer as documented in [13].

As illustrated in fig. 2(b), the controller is very reactive showing a t_{90} of 13 ms for a step of 10 Nm and 35 ms for a step of 40 Nm with only small overshoot.

Disturbance rejection to impulsive loads is evaluated in a collision test. To this end, a pendulum is mounted at the output and the actuator is requested to produce zero torque. The free swinging pendulum is crashed with high velocity into a hard wall and brought to instantaneous rest (ideal plastic collision with a restitution coefficient of zero). Despite high motor speed before the collision, the motor produces only little torque during the impact (fig. 3(a)). In fact, already 2 ms after the collision, the motor maximally decelerates to keep the torque in the spring as small as possible. Due to the motor and gearbox inertia, it takes about 10 ms to bring the motor to a complete rest. If the pendulum collides with the maximal motor velocity, the peak force is smaller than 7 Nm. This implies that whatever collision a system that is built from these joint units experiences, forces occurring at the gear never exceed the peak loads it is rated for. In other words, the drive is perfectly robust against self inflicted collisions.

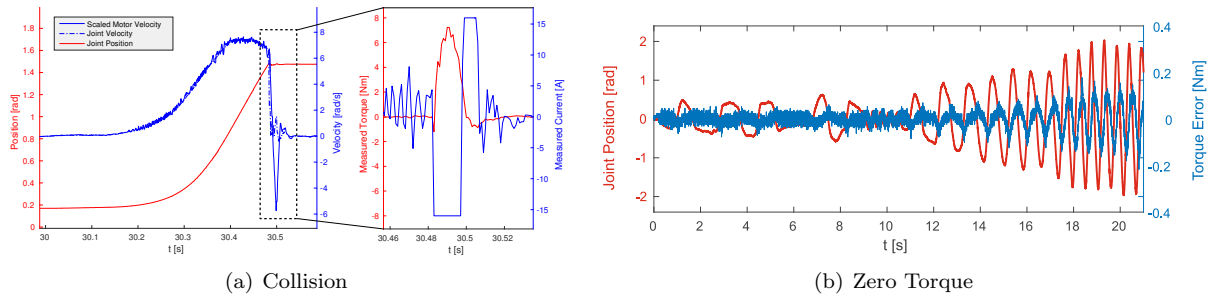|	
(a) Collision	(b) Zero Torque

Figure 3: a) Joint torque during impulsive collision. The motor velocity is scaled with the gear ratio for plotting purposes. b) Zero torque tracking error (blue) when the output joint is randomly moved by hand (red).

As final performance evaluation experiment, the actuator was again commanded to produce zero torque while the output is randomly moved by hand (fig. 3(b)). Despite very large disturbances (2 rad amplitude and about 4 Hz motion), the output torque can be kept at less than 0.2 Nm. A qualitative comparison to Valkyrie and results published in [14] indicates a significantly better disturbance rejection performance.

References

[1] C. Semini, N. G. Tsagarakis, E. Guglielmino, M. Focchi, F. Cannella, and D. G. Caldwell, "Design of HyQ – a hydraulically and electrically actuated quadruped robot," *Proceedings of the Institution of Mechanical Engineers, Part I: Journal of Systems and Control Engineering*, vol. 225, no. 6, pp. 831–849, 2011.

[2] M Raibert, K Blankespoor, G Nelson, and R Playter, "BigDog, the rough-terrain quadruped robot," in *Proceedings of the 17th World Congress*, 2008, pp. 10823–10825.

[3] Boston Dynamics, "ATLAS Robot - http://www.bostondynamics.com/robot_Atlas.html," .

[4] Thiago Cuhna Boaventura, *Hydraulic Compliance Control of the Quadruped Robot HyQ*, Ph.D. thesis, University of Genoa, Italy and Istituto Italiano di Tecnologia (IIT), 2013.

[5] Sangok Seok, Albert Wang, David Otten, and Sangbae Kim, "Actuator design for high force proprioceptive control in fast legged locomotion," in *IEEE/RSJ International Conference on Intelligent Robots and Systems (IROS)*, 2012, pp. 1970–1975.

[6] Sangok Seok, Albert Wang, David Otten, Jeffrey Lang, and Sangbae Kim, "Design principles for highly efficient quadrupeds and implementation on the MIT Cheetah robot," in *IEEE International Conference on Robotics and Automation (ICRA)*, 2013, pp. 3307–3312.

[7] Gill A. Pratt and Matthew M. Williamson, "Series elastic actuators," in *IEEE International Conference on Intelligent Robots and Systems (IROS)*. MIT, 1995, pp. 399–406.

[8] Nicholas Paine, James Holley, Gwendolyn Johnson, and Luis Sentis, "Actuator Control for the NASA-JSC Valkyrie Humanoid Robot : A Decoupled Dynamics Approach for Torque Control of Series Elastic Robots," *Journal of Field Robotics*, 2014.

[9] M Hutter, C Gehring, M Bloesch, M H Hoepflinger, C David Remy, and R Siegwart, "StarlETH: a Compliant Quadrupedal Robot for Fast, Efficient, and Versatile Locomotion," in *International Conference on Climbing and Walking Robots (CLAWAR)*, 2012, pp. 483–490.

[10] Gill A Pratt, Pace Willisson, Clive Bolton, and Andreas Hofman, "Late motor processing in low-impedance robots: impedance control of series-elastic actuators," in *American Control Conference (ACC)*, 2004, vol. 4, pp. 3245–3251.

[11] Nicholas Arden Paine, *High-Performance Series Elastic Actuation*, Ph.D. thesis, The University of Texas at Austin, 2014.

[12] M Hutter, C David Remy, M H Hoepflinger, and R Siegwart, "High Compliant Series Elastic Actuation for the Robotic Leg ScarlETH," in *International Conference on Climbing and Walking Robots (CLAWAR)*, Paris, Fr, 2011, pp. 507–514.

[13] Nicholas Paine, Sehoon Oh, and Luis Sentis, "Design and Control Considerations for High-Performance Series Elastic Actuators," *IEEE/ASME Transactions on Mechatronics*, vol. 19, no. 3, pp. 1080–1091, June 2014.

[14] Nicolaus A. Radford, Philip Strawser, Kimberly Hambuchen, Joshua S. Mehling, William K. Verdeyen, A. Stuart Donnan, James Holley, Jairo Sanchez, Vienny Nguyen, Lyndon Bridgwater, Reginald Berka, Robert Ambrose, Mason Myles Markee, N. J. Fraser-Chanpong, Christopher Mc-Quin, John D. Yamokoski, Stephen Hart, Raymond Guo, Adam Parsons, Brian Wightman, Paul Dinh, Barrett Ames, Charles Blakely, Courtney Edmondson, Brett Sommers, Rochelle Rea, Chad Tobler, Heather Bibby, Brice Howard, Lei Niu, Andrew Lee, Michael Conover, Lily Truong, Ryan Reed, David Chesney, Robert Platt, Gwendolyn Johnson, Chien-Liang Fok, Nicholas Paine, Luis Sentis, Eric Cousineau, Ryan Sinnet, Jordan Lack, Matthew Powell, Benjamin Morris, Aaron Ames, and Jide Akinyode, "Valkyrie: NASA's First Bipedal Humanoid Robot," *Journal of Field Robotics*, vol. 32, no. 3, pp. 397–419, May 2015.

[15] M Bloesch, M Hutter, M Hoepflinger, S Leutenegger, C Gehring, C David Remy, and R Siegwart, "State Estimation for Legged Robots - Consistent Fusion of Leg Kinematics and IMU," in *Robotics Science and Systems (RSS)*, 2012, pp. 17–24.

[16] Michael Bloesch, Christian Gehring, Peter Fankhauser, Marco Hutter, Mark A. Hoepflinger, and Roland Siegwart, "State estimation for legged robots on unstable and slippery terrain," in *IEEE/RSJ International Conference on Intelligent Robots and Systems (IROS)*, 2013, pp. 6058–6064.

[17] Miomir Vukobratovic and Davor Juricic, "Contribution to the synthesis of biped gait," *Biomedical Engineering, IEEE Transactions on*, , no. 1, pp. 1–6, 1969.

[18] R B McGhee, "Some finite state aspects of legged locomotion," *Mathematical Biosciences*, vol. 2, no. 1-2, pp. 67–84, 1968.

[19] Christian Gehring, Stelian Coros, Marco Hutter, Michael Bloesch, Péter Fankhauser, Mark Hoepflinger, and Roland Siegwart, "Towards Automatic Discovery of Agile Gaits for Quadrupedal Robots," in *IEEE International Conference on Robotics and Automation (ICRA)*, 2014, pp. 4243–4248.

[20] M Hutter, H Sommer, C Gehring, M. Hoepflinger, M Bloesch, and R Siegwart, "Quadrupedal locomotion using hierarchical operational space control," *The International Journal of Robotics Research (IJRR)*, vol. 33, no. 8, pp. 1062–1077, May 2014.

[21] Christian Gehring, C. Dario Bellicoso, Huub Heijnen, Remo Diethelm, Peter Fankhauser, Michael Bloesch, Jemin Hwangbo, Markus A. Hoepflinger, Stelian Coros, Roland Siegwart, and Marco Hutter, "An Optimization Approach to Robust Control of Dynamic Motions with a Compliant Quadrupedal Robot," *IEEE Robotics and Automation Magazine Special Issue on Bioinspired Motor Control for Articulated Robots*, 2015.

[22] Marco Hutter, Christian Gehring, Mark A. Hopflinger, Michael Blosch, and Roland Siegwart, "Toward Combining Speed, Efficiency, Versatility, and Robustness in an Autonomous Quadruped," *IEEE Transactions on Robotics*, vol. 30, no. 6, pp. 1427–1440, Dec. 2014.

[23] C David Remy, Oliver Baur, Martin Latta, Andi Lauber, M Hutter, M H Hoepflinger, C Pradalier, and R Siegwart, "Walking and crawling with ALoF: a robot for autonomous locomotion on four legs," *Industrial Robot: An International Journal*, vol. 38, no. 3, pp. 264–268, 2011.